

Article

Cr(VI) Adsorption from Aqueous Solution by UiO-66 Modified Corncob

Hongzhong Xie^{1,2}, Yanlei Wan^{1,3}, Hao Chen^{1,4}, Guangcheng Xiong¹, Lingqing Wang⁵ , Qi Xu¹, Xiang Li¹ and Qihong Zhou^{1,*}

- ¹ Changjiang Institute of Survey, Planning, Design and Research Co., Ltd., Wuhan 430010, China; xiehongzhong@cjwsjy.com.cn (H.X.); wanyanlei@cjwsjy.com.cn (Y.W.); chenhao@cjwsjy.com.cn (H.C.); xiongguangcheng@cjwsjy.com.cn (G.X.); xuqi3@cjwsjy.com.cn (Q.X.); lixiang6@cjwsjy.com.cn (X.L.)
- ² Hubei Provincial Engineering Research Center for Comprehensive Water Environment Treatment in the Yangtze River Basin, Wuhan 430010, China
- ³ Key Laboratory of Changjiang Regulation and Protection of Ministry of Water Resources, Wuhan 430010, China
- ⁴ Hubei Key Laboratory of Basin Water Security, Wuhan 430010, China
- ⁵ Key Laboratory of Land Surface Pattern and Simulation, Institute of Geographical Sciences and Natural Resources Research, Chinese Academy of Sciences, Beijing 100101, China; wanglq@igsrr.ac.cn
- * Correspondence: zhouqihong@cjwsjy.com.cn

Abstract: To adsorb hexavalent chromium (Cr(VI)) in polluted water, this paper prepared a UiO-66 (Zr₆O₄(OH)₄(BDC)₁₂) modified granular corncob composite adsorbent by hydrothermal method with in situ loading of UiO-66 on pretreated corncob particles. The physicochemical properties of the synthesized samples were characterized. Batch adsorption experiments were conducted to investigate the adsorption process of aqueous Cr(VI) under various conditions (different ionic strength, pH and co-existing anions). The results showed that UiO-66 was successfully loaded on the modified corncob particles. The isothermal adsorption data of Cr(VI) adsorption by the UiO-66 modified corncob fit well with the Langmuir model with the maximum adsorption capacity of Cr(VI) on UiO-66@Corn⁺ being 90.04 mg/g. UiO-66 loading could increase Cr(VI) adsorption capacity of Corn⁺. The kinetic study showed that the equilibrium time for Cr(VI) adsorption on UiO-66 modified corncob was about 180 min and the kinetic data followed the pseudo-secondary kinetic model. The Cr(VI) adsorption capacity on UiO-66@Corn⁺ decreased with the increasing solution pH, and the optimum pH range was 4–6. The ionic strength has little effect on the Cr(VI) adsorption capacity, but the coexistence of CO₃²⁻, SO₄²⁻ and PO₄³⁻ in the solution could significantly decrease the equilibrium adsorption capacity of Cr(VI). The adsorption mechanism analysis showed that Cr(VI) was adsorbed on the surface of adsorbents through electrostatic attraction and was reduced further to the less toxic Cr(III) by the electron donor on the surface of adsorbent. The electrostatic interaction was the main force affecting the adsorption of Cr(VI) by UiO-66. UiO-66@Corn⁺ had an excellent removal efficiency of Cr(VI) and excellent reusability. UiO-66@Corn⁺ could effectively remove Cr(VI) from water and have a promising application.

Keywords: UiO-66; corncob; adsorption; Cr(VI); agricultural wastes



Citation: Xie, H.; Wan, Y.; Chen, H.; Xiong, G.; Wang, L.; Xu, Q.; Li, X.; Zhou, Q. Cr(VI) Adsorption from Aqueous Solution by UiO-66 Modified Corncob. *Sustainability* **2021**, *13*, 12962. <https://doi.org/10.3390/su132312962>

Academic Editors: Hefa Cheng and Xiande Xie

Received: 29 September 2021
Accepted: 15 November 2021
Published: 23 November 2021

Publisher's Note: MDPI stays neutral with regard to jurisdictional claims in published maps and institutional affiliations.



Copyright: © 2021 by the authors. Licensee MDPI, Basel, Switzerland. This article is an open access article distributed under the terms and conditions of the Creative Commons Attribution (CC BY) license (<https://creativecommons.org/licenses/by/4.0/>).

1. Introduction

Chromium (Cr) usually exists as Cr(III) or Cr(VI), and the toxicity of Cr(VI) is much greater than that of Cr(III) [1]. Cr(VI) is commonly found in industrial wastewater such as textiles, electroplating, leather production, cooling towers and metal processing. A small amount of Cr(VI) could have the risk of carcinogenesis and teratogenesis to humans and animals. Cr(VI) has been recognized as one of the most toxic heavy metals by the International Agency for Research on Cancer (IARC) [2]. The US Environmental Protection Agency (USEPA) stipulates that the maximum permissible concentration of chromium in drinking water is 0.1 mg/L. The WHO requires that Cr(VI) concentration in drinking water

should be less than 0.05 mg/L. Due to the widespread use of Cr(VI) in the industry, a large amount of Cr(VI) from industrial wastewater and municipal sewage enters natural water bodies, which harms the ecological environment and threatens the safety of drinking water. Therefore, it is important to remove Cr(VI) from water effectively.

Various technologies such as adsorption, membrane technology, electrochemical precipitation, chemical coagulation, redox, bioremediation and ion exchange have been tested for Cr(VI) removal from water [3,4]. Among these technologies, adsorption is considered the most cost-effective technique for Cr(VI) polluted water treatment due to its simple operation, low cost and high efficiency. Therefore, numerous adsorbents have been used to remove Cr(VI) from water in recent years, such as activated carbon, chitosan, metal (hydrogen) oxide and clay minerals [5–7]. However, these adsorbents with low adsorption capacity can be easily agglomerated during the adsorption process and cause difficulty in solid-liquid separation. In addition, precise control of the physical and chemical properties of the adsorbent for specific pollutants is also a challenging problem.

Metal-organic frameworks (MOFs) are new porous materials with adjustable pore structure, designable surface functional groups, high porosity and large specific surface area [8]. MOFs have received extensive attention in energy storage, drug delivery, gas adsorption and storage, catalysis and water pollution remediation [9–13]. ZIF-8, MIL-100 and Zr-based MOFs (such as UiO-66) have attracted attention in water pollution control due to their high bonding strength, stable structure and high-water stability. UiO-66 is composed of $Zr_6O_4(OH)_4$ nodes and twelve terephthalate (BDC) ligands. There are six Zr^{4+} in the octahedral geometry of $Zr_6O_4(OH)_4$ and four oxygen atoms or hydroxyls in the center of each interface of the octahedron. These metal nodes are coordinated with twelve BDC ligands [14]. The theoretical pore volume and the theoretical specific surface area of UiO-66 are $0.45 \text{ cm}^3/\text{g}$ and $1018 \text{ m}^2/\text{g}$, respectively. UiO-66 has excellent structural stability, thermal stability and mechanical strength [14]. UiO-66 has been reported in the literature for the removal of dyes and heavy metals in water. Wang et al. reported that UiO-66 can form a covalent bond with As(V) through the hydroxyl function group to remove arsenic from water [15]. Li et al. used a silver-triazolato framework to remove Cr(VI) from water and the results showed that it displayed a fast, efficient and reversible adsorption of Cr(VI), the maximum adsorption capacity (q_m) could be up to 37.0 mg/g [16]. Sun et al. synthesized ultra-stable Zr-MOF (JLU-MOF50), which exhibited a commendable trapping capacity (92.0 mg/g) and a fast adsorption rate ($32.5 \text{ mg}/(\text{g min})$) [17]. In addition to their lower hydrothermal stability, another important reason is that MOFs are usually micron powder and have low mechanical strength, making them easy to wash away and difficult to be separated from water. High-pressure drop and easy agglomeration are also the problems that must be solved in the practical engineering application of MOFs such as UiO-66. Thus, MOFs have not been used in actual waste-water treatment. It is possible to effectively solve this problem by attaching the MOFs particles in porous host materials with larger sizes [18].

A large amount of agricultural waste is generated during agricultural production. China annually produces about 900 million tons of agricultural waste, and it is increasing yearly at a rate of 5–10%. However, most of them are not properly utilized [19]. Direct abandonment and incineration are common methods for people to dispose agricultural waste. During the incineration process, harmful substances such as carbon dioxide, carbon monoxide, sulfur dioxide and dust are released into the air, contributing to the greenhouse effect, air pollution and respiratory diseases. The technique of resource utilization of agricultural waste is needed urgently.

In this paper, agricultural waste corncob was used as the host material. Firstly, the corncob was modified, and then the UiO-66 loading corncob was prepared by hydrothermal method. Its physical and chemical properties were analyzed through various characterization methods. The adsorption characteristics for Cr(VI) was systematically explored. The removal mechanism of Cr(VI) from aqueous solution by synthesized UiO-66 loading corncob was studied.

2. Materials and Methods

2.1. Materials

The chemicals including sodium hydroxide (AR), ethanol (AR), chloroacetic acid (AR), N,N-dimethylformamide (DMF, AR), epichlorohydrin (AR), ethylenediamine (AR), triethylamine (AR), zirconium tetrachloride (AR), 1,4-dicarboxybenzene acid (AR), methanol (AR), sodium chloride (AR), Sodium nitrate (AR), sodium carbonate (AR), sodium phosphate (AR), sodium sulfate (AR), potassium dichromate (GR), nitric acid (GR) and hydrochloric acid (GR), which were purchased from Sinopharm Chemical Reagent Co. Ltd. Corncob pellets (≤ 0.6 mm) were obtained from Dezhou in the Shandong province (China). The Chromium standard solution (GSB04-1723-2004(a)) was purchased from the National Non-ferrous Metals and Electronic Materials Analysis and Testing Center (China). Deionized water was produced by a laboratory ultrapure water machine (UPC-III-10T, Sichuan Youpu).

2.2. Synthesis of UiO-66 Modified Corncob

UiO-66 modified corncob was synthesized by a modified method [20]. Briefly, 20 g of dried corncob was added to 250 mL NaOH (10 wt%) ethanol and water (V:V = 1:2) solution and the suspension was stirred at room temperature for 1 h. Then, the mixed solution was heated to 90 °C, after which 100 mL of 50 wt% chloroacetic acid solution was added, then stirred at 80 °C for 1.5 h and cooled to room temperature. After filtering, the sample was first washed with 0.2 mol/L NaOH and 0.2 mol/L HCl and then washed with deionized water to neutrality, before being dried at 50 °C for 24 h to obtain a corncob with a negatively charged surface (Corn⁻). Next, 20 g of dried corncob was added to 175 mL of N-dimethylformamide (DMF) and stirred at room temperature for 2 h. Then, 25 mL of epichlorohydrin was added to the mixture and stirred at 85 °C for 1 h. Then, 10 mL of ethylenediamine and 50 mL of triethylamine (grafted with quaternary amino groups on the surface of the corncob) were added dropwise during the stirring and continued to be stirred at 85 °C for 4 h. After the reaction, corncob pellets were collected through filtration. The samples were washed sequentially with 0.2 mol/L NaOH and 0.2 mol/L HCl solutions and finally with deionized water. Samples were dried at 50 °C for 24 h to obtain a corncob with a positive charge on the surface (Corn⁺). Next, 1 g ZrCl₄ was dissolved in 75 mL DMF and ultrasonically treated for 30 min, and 0.7 g terephthalic acid was dissolved in 25 mL DMF and this solution was added to the ZrCl₄ solution. A measure of 1 g Corn⁺ or Corn⁻ was added into the mixed solution. After being stirred for 30 min, the mixed solution was transferred to a 150 mL Teflon-lined stainless autoclave and reacted at 110 °C for 24 h. After, the solid products were collected and washed three times with DMF or methanol and dried at 50 °C for 24 h to obtain UiO-66@Corn⁺ or UiO-66@Corn⁻.

2.3. Characterization

The X-ray diffraction (XRD) spectrum of the sample was analyzed by an X-ray diffractometer (Bruker D8 ADVANCE) with the Cu K α radiation and scanning range of 5°~85°. The microscopic morphologies of the samples were observed by a field emission scanning electron microscope (Thermo scientific Apreo 2C). The elemental chemical analysis was performed using the energy-dispersive X-ray analysis (EDS) system attached to the SEM instrument. The functional groups in the sample were analyzed by Fourier infrared spectroscopy (FTIR, Thermo Fisher Nicolet Is5-transmission/ATR mode). The element's content and morphology of the sample surface were analyzed by X-ray photoelectron spectroscopy (XPS, ThermoFisher Escalab Xi + Al target (full spectrum + narrow scan)) with a test Passing-Energy of full spectrum of 100 eV, narrow scan of 30 eV, step length of 0.1 eV and residence time of 40–50 ms. The concentration of Cr(VI) in water was measured by an inductively coupled plasma spectrometer (ICP-5000, Concentrator Technology).

2.4. Adsorption Experiments

Adsorption kinetics study: Cr(VI) sorption dynamics were carried out by adding 0.1 g adsorbents to a 100 mL 40 mg/L Cr(VI) aqueous solution (pH = 6.5 \pm 0.2) in a 250 mL

conical flask. Unless otherwise specified, the pH of the Cr(VI) aqueous solution in all adsorption experiments was controlled at 6.5 ± 0.2 . The mixed solution was shaken at 25°C and 120 r/min. A series of contact time (5, 15, 30, 60, 120, 180, 300, 500, 900 and 1500 min) was set. After each contact time, 20 mL of the solution was filtered with a 0.45 μm syringe filter, and the content of Cr(VI) in the filtrate was analyzed by ICP.

Adsorption equilibrium experiment: The adsorption capacities of virgin corncob, Corn^+ , Corn^- , UiO-66@Corn^- , UiO-66@Corn^+ and UiO-66 for Cr(VI) were evaluated by batch Cr(VI) adsorption experiments. A measure of 0.1 g adsorbent was added to the 100 mL solution with Cr(VI) concentration of 0~150 mg/L ($\text{pH} = 6.5 \pm 0.2$). The mixed solution was shaken at 25°C 120 r/min for 12 h. After filtration, the concentration of Cr(VI) in the filtrate was analyzed.

Effects of solution environment: The effect of solution pH on Cr(VI) adsorption by UiO-66@Corn^+ was carried out by adding 0.1 g UiO-66@Corn^+ in 100 mL 40 mg/L Cr(VI) solution with the pH varying from 3.0 to 12.0. The mixed solution was shaken at 25°C 120 r/min for 12 h, then the solution was filtered and the content of Cr(VI) in the filtrate was measured. The effect of ionic strength on the adsorption of Cr(VI) by UiO-66@Corn^+ was conducted by adding different concentrations of NaCl (0.01, 0.1, 0.3 and 0.5 mol/L) during the adsorption experiment. The effect of coexisting anions on the adsorption of Cr(VI) by UiO-66@Corn^+ was operated by adding 0.05 mol/L NaNO_3 , Na_2CO_3 , Na_2SO_4 or Na_3PO_4 to the 100 mL 40 mg/L Cr(VI) solution ($\text{pH} = 6.5 \pm 0.2$).

Regeneration studies: To evaluate the reusability of UiO-66@Corn^+ , 0.1 g of used UiO-66@Corn^+ was collected and eluted with different concentrations (0.01, 0.1, 0.5 mol/L) of NaOH solutions for 12 h. After washing with ultrapure water several times, the UiO-66@Corn^+ was added to the 100 mL 40 mg/L Cr(VI) solution at pH 6.5. The mixed solution was shaken at 25°C 120 r/min for 12 h, then the solution was filtered and the content of Cr(VI) in the filtrate was measured to determine the optimal NaOH concentration. The adsorption-desorption process was repeated five times with the optimal NaOH concentration.

2.5. Data Analysis

The Cr(VI) adsorption capacity and remove efficiency were calculated by the following Equations [21]:

Adsorption capacity:

$$q_e = \frac{(C_0 - C_e) \times V}{m} \quad (1)$$

Remove efficiency:

$$R_e = \frac{(C_0 - C_e) \times 100}{C_0} \quad (2)$$

where q_e was the equilibrium adsorption capacity of Cr(VI) (mg/g), C_0 was the initial concentration of Cr(VI) (mg/L), C_e was the concentration of Cr(VI) at equilibrium (mg/L), V was the volume of the solution (L), m was the amount of the adsorbent added (g) and R_e was the remove efficiency of Cr(VI) (%).

Kinetic models (pseudo-first-order model (Equation (3)), pseudo-second-order (Equation (4)) and intra-particle diffusion model (Equation (5)) [22,23], were applied to describe different steps involved in the Cr(VI) adsorption process.

$$\ln(q_e - q_t) = \ln q_e - k_1 t \quad (3)$$

$$\frac{t}{q_t} = \frac{1}{k_2 q_e^2} + \frac{t}{q_e} \quad (4)$$

$$q_t = k_{pi} t^{1/2} + c \quad (5)$$

where q_e and q_t are the Cr(VI) adsorption capacity (mg/g) at equilibrium moment and time t (min), k_1 and k_2 are the rate constant of the pseudo-first-order (1/min) and pseudo-second-

order model (g/(mg min)). k_{pi} (mg/(g min)^{0.5}) is the rate constant of intraparticle diffusion, and c is associated with the thickness of the boundary layer at each adsorption stage.

Adsorption isotherms were conducted to study the adsorption behavior of Cr(VI) on synthesized adsorbents. The experimental equilibrium data were fitted by the Freundlich (Equation (6)), Langmuir (Equation (7)) and Langmuir-Freundlich models (Equation (8)).

The Freundlich model [24]:

$$q_e = K_F C_e^{1/n} \quad (6)$$

where q_e is the equilibrium adsorption capacity of Cr(VI) (mg/g), C_e is the Cr(VI) concentration in solution at equilibrium moment (mg/L), K_F is the Freundlich constant related to the sorption affinity and $1/n$ is the Freundlich exponential coefficient.

The Langmuir model [25]:

$$q_e = \frac{q_m K_L C_e}{1 + K_L C_e} \quad (7)$$

where q_m is the maximum adsorption capacity of Cr(VI) (mg/g) and K_L is the Langmuir constant refer to the adsorption affinity (L/mg).

The Langmuir-Freundlich model [26]:

$$q_e = \frac{Q_g (K_{LF} C_e)^n}{1 + (K_{LF} C_e)^n} \quad (8)$$

where Q_g is the Cr(VI) maximum adsorption capacity (mg/g), K_{LF} is the Langmuir-Freundlich constant related to the adsorption affinity and n is the relating to the heterogeneity of adsorbent surface.

The experimental data in this paper were processed and analyzed by Origin 9.0 and Jade 6.0.

3. Results and Discussion

3.1. Characterization of UiO-66 Modified Corncob

Figure 1 displays the general SEM images of the corncob and the UiO-66 modified corncob. The surface of the virgin corncob is relatively smooth with a small amount of pore structure (Figure 1a,b). The surface of the UiO-66@Corn⁻ was loaded with a small amount of fragments and particles (Figure 1c), and the pore structure was more abundant than the virgin corncob (Figure 1d). Compared to the virgin corncob and the UiO-66@Corn⁻, the surface of UiO-66@Corn⁺ was more porous and loaded with more UiO-66 particles (Figure 1e,f). The UiO-66 showed irregular agglomeration, which was consistent with a previous study [27]. The SEM pictures indicated that after the Corn⁺ treatment, the corncob pore structure was more abundant and more UiO-66 could be loaded. The EDS element content analysis also showed that the Zr content in UiO-66@Corn⁺ (2.95%) was higher than in UiO-66@Corn⁻ (1.53%) (Table S1 in Supplementary Materials), which was in accordance with the XPS element results: the Zr content in UiO-66@Corn⁺ was 2.02% and in the UiO-66@Corn⁻ it was 1.31%.

XRD patterns of the virgin corncob, UiO-66, used UiO-66, Corn⁺, Corn⁻, UiO-66@Corn⁺ and UiO-66@Corn⁻ are shown in Figure 2. The peaks at 7.4 and 8.5 are characteristic peaks of UiO-66, which verified that UiO-66 was successfully synthesized. They are also appeared on UiO-66@Corn⁺ which indicated that UiO-66 was loaded on Corn⁺. The characteristic peaks of UiO-66 did not appear on UiO-66@Corn⁻, presumably because the loading was too low. The peaks on UiO-66 and used UiO-66 was similar, indicating that the UiO-66 was very stable during the Cr(VI) adsorption process. The broad peak at about $2\theta = 22.1^\circ$ appeared on the virgin corncob, Corn⁺, Corn⁻, UiO-66@Corn⁺ and UiO-66@Corn⁻ and was standing for the amorphous state of the corncob.

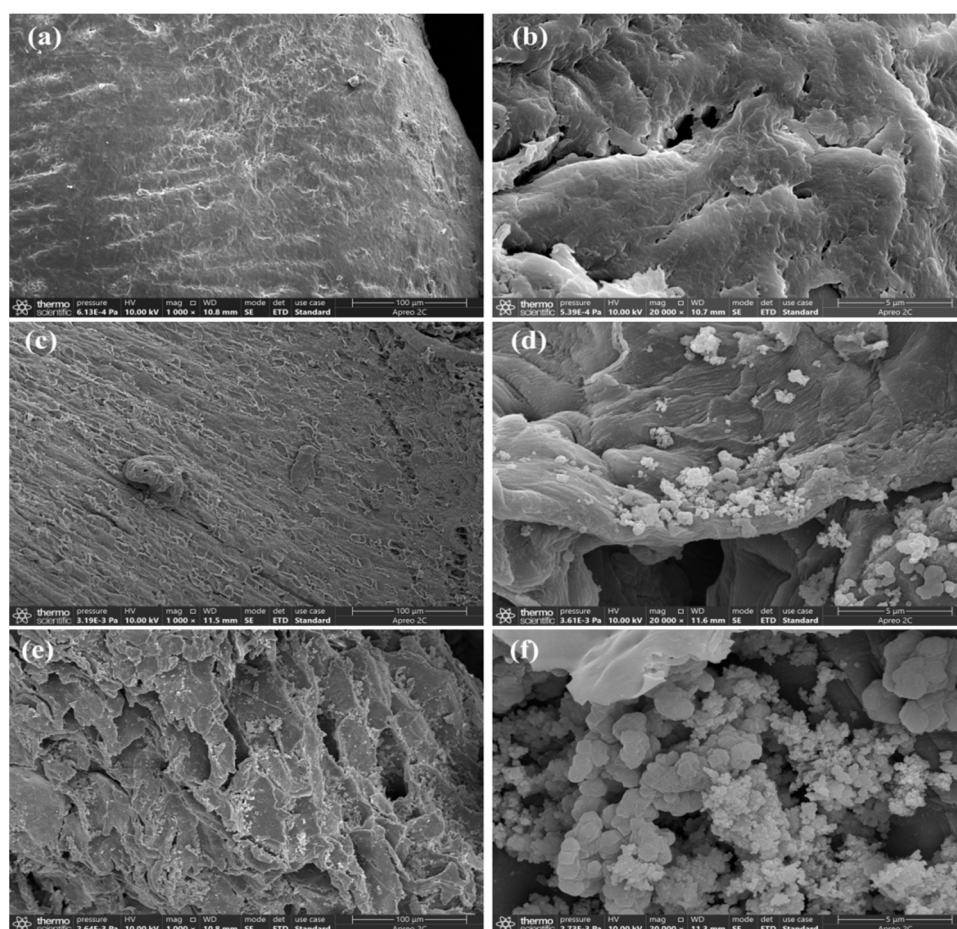


Figure 1. SEM images of synthesized UiO-66 modified corncob: (a,b) corncob; (c,d) UiO-66@Corn⁻; (e,f) UiO-66@corn⁺.

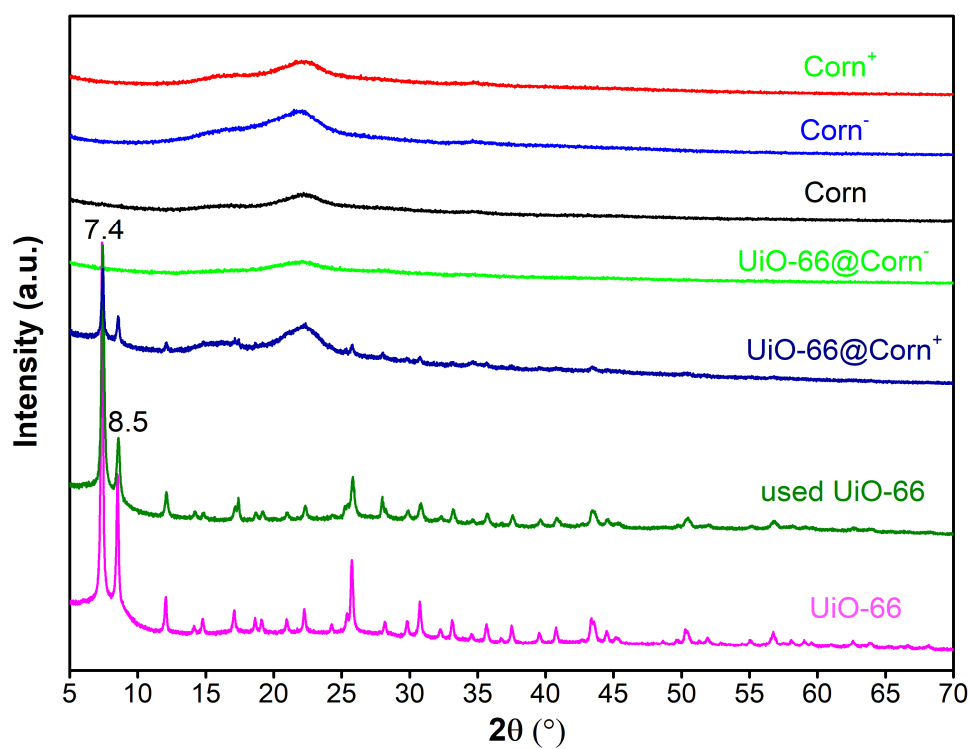


Figure 2. XRD patterns of corncob and synthesized UiO-66 modified corncob.

3.2. Adsorption Kinetics

Adsorption kinetics of Cr(VI) by UiO-66@Corn⁺ and UiO-66@Corn⁻ were studied, and the results were shown in Figure 3. At the beginning, the adsorption loading and removal efficiency of Cr(VI) increased rapidly with time. After about 180 min, the adsorption loading and removal efficiency of Cr(VI) reached equilibrium. The equilibrium time of Cr(VI) on the two adsorbents was similar. The equilibrium time of isotherm adsorption was set at 12 h and was enough for Cr(VI) adsorption to reach equilibrium. The equilibrium adsorption capacity of Cr(VI) on UiO-66@Corn⁺ was about three times greater than that on UiO-66@Corn⁻. The process of adsorbate in the solution reaching the adsorption sites on adsorbent is usually divided into three stages [28,29]: (1) membrane diffusion or boundary layer diffusion, which refers to the diffusion of the adsorbate from the solution to the outer surface of the adsorbent; (2) intra-particle diffusion, also known as capillary diffusion, which refers to the adsorbate molecules enter the internal pores of the adsorbent from the boundary layer; (3) adsorbent molecules attaching to the active sites of the adsorbent through physical and chemical reactions. The pseudo-first-order kinetic model, pseudo-second-order kinetic model and intra-particle diffusion model were used to fit the kinetic data. The kinetic parameters are summarized in Table 1. The adsorption kinetic curves of Cr(VI) on the two adsorbents were well fitted with the pseudo-second-order kinetic model (R^2 values ≥ 0.999), indicating that the Cr(VI) adsorption that occurred on UiO-66@Corn⁺ and UiO-66@Corn⁻ were mainly chemical adsorption. Previous studies have shown that there were two adsorption mechanisms of Cr(VI) on the adsorbent: one was that Cr(VI) was reduced to Cr(III) on the surface of the adsorbent, then Cr(III) was adsorbed; the other was that Cr(VI) directly adsorbed on adsorbent [30]. Therefore, it is speculated that the process of UiO-66 modified corncob adsorption of Cr(VI) may contain the process of reducing Cr(VI) to Cr(III). The relevant adsorption mechanism will be further discussed in a later section.

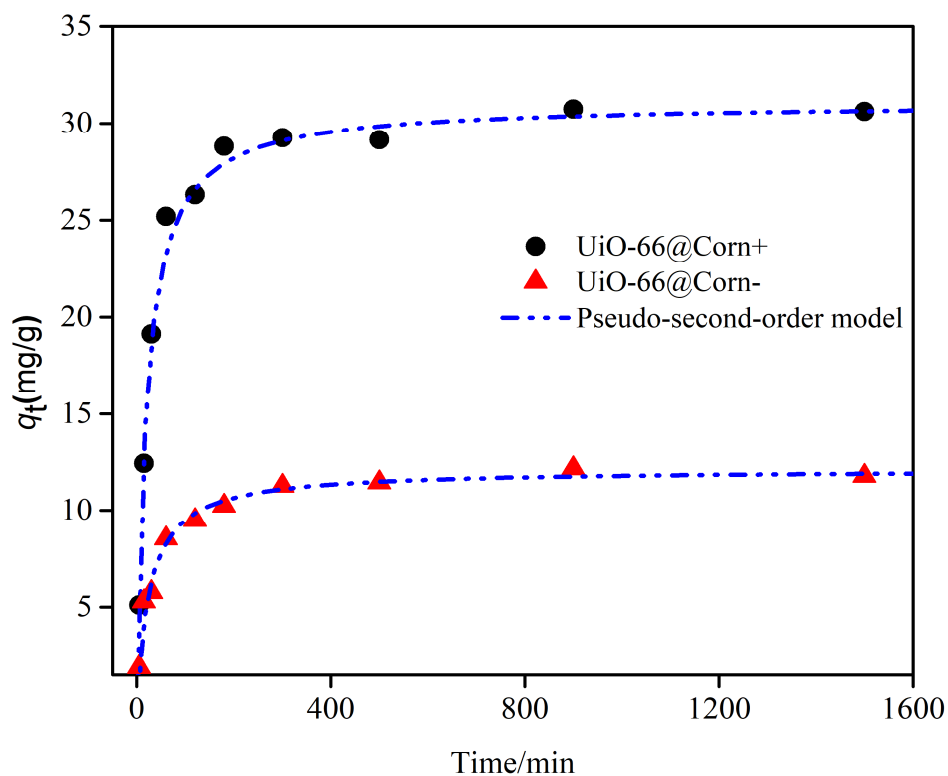


Figure 3. Kinetic study of Cr(VI) adsorption on UiO-66 modified corncob.

Table 1. Kinetic models parameters for the adsorption of Cr(VI) on UiO-66 modified corncob.

Adsorbents	$q_{e,exp}$ (mg/g)	Pseudo-First-Order Model			Pseudo-Second-Order Model			Intra-Particle Diffusion Model		
		K_1 (min ⁻¹)	$q_{e,calculated}$ (mg/g)	R^2	K_2 (g/(mg·min))	$q_{e,calculated}$ (mg/g)	R^2	k_{pi} (mg/(g·min ^{0.5}))	c	R^2
UiO-66@Corn ⁺	30.621	0.003	8.802	0.813	0.002	31.056	1.000	0.540	15.473	0.550
UiO-66@Corn ⁻	12.166	0.002	4.180	0.665	0.003	12.110	0.999	0.231	5.275	0.657

3.3. Cr(VI) Adsorption Equilibrium

To study the adsorption process and mechanism, the experimental data of adsorption isotherm were fitted by the Langmuir model (LM), Freundlich model (FM) and Langmuir–Freundlich model (LFM). The fitting parameters were calculated and presented in Table 2. The Langmuir model assumes that the adsorption process is monolayer adsorption, the surface of the adsorbent is uniform, and the adsorption sites are limited. The Freundlich model usually assumes that the adsorption process is multi-layer adsorption and that there is more than one interaction between the adsorbent and the adsorbate. Generally, smaller $1/n$ value in the Freundlich model means easier adsorption, when $1/n < 1$, the adsorption is prone to occur. The larger the K_L in the Langmuir model, the stronger the adsorption affinity. The maximum adsorption capacities of Cr(VI) on UiO-66, Corn⁺, UiO-66@Corn⁺ and UiO-66@Corn⁻ were 109.88 mg/g, 60.232 mg/g, 90.038 mg/g and 22.383 mg/g, respectively (Table 2). It can be inferred from the value of $1/n$ that the adsorption processes of Cr(VI) on the four adsorbents were easy to occur. It is easier to adsorb on UiO-66@Corn⁻, and Cr(VI) has a higher adsorption affinity on UiO-66@Corn⁻. According to the correlation coefficient (R^2), the Langmuir model and the Langmuir–Freundlich model could well fit the adsorption data. The results indicated that the process of Cr(VI) adsorption on UiO-66 and UiO-66 modified corncobs tend to be monolayer adsorption, the adsorption capacity of Cr(VI) is closely related to the number of adsorption sites and the specific surface area of the adsorbent.

Table 2. Equilibrium parameters for the Cr(VI) adsorption on UiO-66 and UiO-66 modified corncobs.

Adsorbents	Langmuir Model			Freundlich Model			Langmuir–Freundlich Model			
	K_L (L/mg)	q_m (mg/g)	R^2	$1/n$	K_F (L/g)	R^2	Q_g (mg/g)	K_{LF} (L/mg)	n	R^2
Corn ⁺	0.053	60.232	0.993	0.452	6.944	0.950	54.971	0.066	1.175	0.994
UiO-66	0.031	109.88	0.990	0.484	9.334	0.961	102.00	0.037	1.115	0.989
UiO-66@Corn ⁺	0.032	90.038	0.993	0.565	5.810	0.975	84.940	0.037	1.059	0.992
UiO-66@Corn ⁻	0.066	22.383	0.990	0.470	2.787	0.939	19.539	0.090	1.272	0.994

The isotherm curves are shown in Figure 4. It was clear that the adsorption capacity of Cr(VI) on corn and Corn⁻ were very low. The equilibrium adsorption capacity (q_e) of Cr(VI) on UiO-66, Corn⁺, UiO-66@Corn⁺ and UiO-66@Corn⁻ both increased with the Cr(VI) equilibrium concentration and then slowly reached equilibrium (Figure 4). While the removal efficiency (R_e) of Cr(VI) on these adsorbents gradually decreased as the Cr(VI) equilibrium concentration increased. The adsorption isotherm curves of Cr(VI) on the four adsorbents belonged to the “L” shape, and the equilibrium adsorption capacity of Cr(VI) on the four adsorbents followed UiO-66 > UiO-66@Corn⁺ > Corn⁺ > UiO-66@Corn⁻. UiO-66 has the highest adsorption capacity for Cr(VI) (109.88 mg/g). The adsorption capacity of Cr(VI) by Corn⁺ was 60.232 mg/g, after loaded with UiO-66, it increased to 90.038 mg/g. Therefore, UiO-66 loading can significantly increase the adsorption capacity of Cr(VI) by Corn⁺.

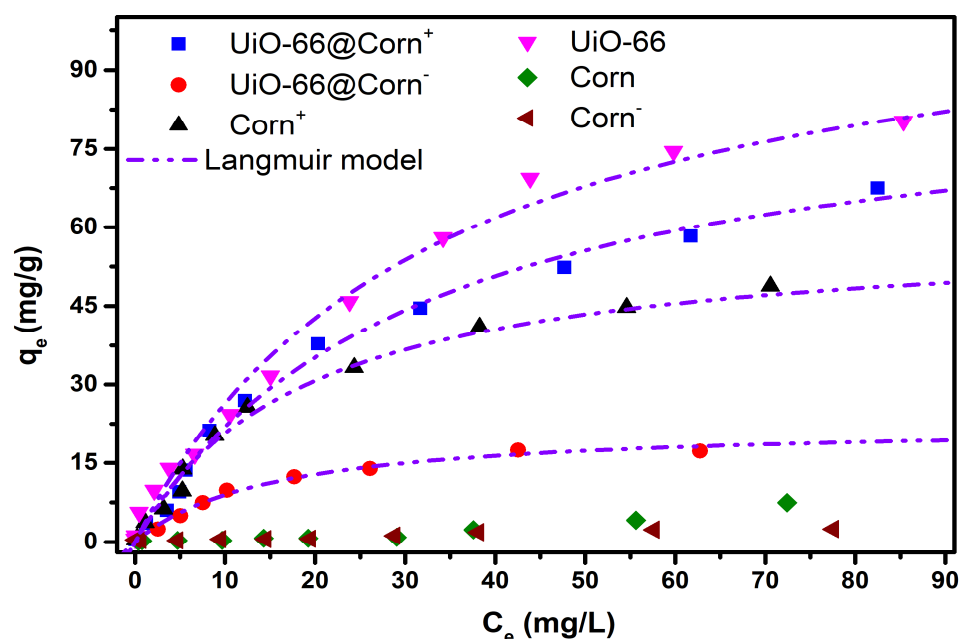


Figure 4. Adsorption isotherms of Cr(VI) by UiO-66 and UiO-66 modified corncob.

Table 3 lists the maximum adsorption capacity (q_m) of Cr(VI) on different adsorbents. Obviously, the q_m of Cr(VI) on UiO-66@Corn⁺ synthesized in this study exceeds most adsorbents reported in the literature in recent years. Therefore, UiO-66@Corn⁺ is a cost-effective adsorbent, which has broad prospect in eliminating Cr(VI) from water.

Table 3. Adsorption capacity of Cr(VI) on different adsorbents (mg/g).

Adsorbents	q_m	Reference	Adsorbents	q_m	Reference
Ce-UiO-66	30.00	[2]	TiO ₂ -Ag	25.70	[31]
EDTA-chitosan/Cu-BTC	46.51	[32]	CaAl-CO ₃ LDH	20.24	[33]
UiO-66	36.40	[34]	Rice husk	25.2	[35]
UiO-66-(OH) ₂	59.20	[34]	GO-NiFe LDH	53.6	[36]
CoMgAl-LDH	59.27	[37]	Wool keratin/PET composite	75.86	[38]
MSS	46.08	[39]	MOF-867	53.4	[40]
MnO ₂ -deposited diatomites	48.2	[41]	UiO-66@Corn ⁺	90.04	This study
Modified montmorillonite	43.84	[42]	UiO-66@Corn ⁻	22.38	This study

3.4. Effects of Solution Chemistry

The adsorption behavior of Cr(VI) on UiO-66@Corn⁺ differed in solutions of different pH. The pH value of the solution can change the surface charges and the type of functional groups of the adsorbent through protonation and deprotonation, which in turn has an important impact on its adsorption behavior. In addition, the solution pH will also affect the ionic form of the heavy metals [31]. As shown in Figure 5a, with increasing solution pH, the adsorption capacity of Cr(VI) on UiO-66@Corn⁺ increased, reaching its maximum value at pH 5 and then decreased as the pH value increased. The adsorption capacity of Cr(VI) by UiO-66@Corn⁺ increased from 33.30 mg/g to 37.23 mg/g when the pH value was raised from 3 to 5 and then dropped gradually to 28.35 mg/g with the pH raising to 9, before further dropping sharply to 4.45 mg/g after the pH changed from 9 to 11. In the aqueous solution, the Cr(VI) generally existed in the form of Cr₂O₇²⁻ (2 < pH < 6), H₂CrO₄ (pH < 1), HCrO₄⁻ (2 < pH < 6), CrO₄²⁻ (pH > 6.8) in different proportions, which depended on the pH value of the solution [43]. It is clear that when Cr(VI) exists in the form of CrO₄²⁻, double the number of active adsorption sites were required to remove Cr(VI) from the aqueous solution. The p*H*_{pzc} of UiO-66@Corn⁺ is about 5.86 (Figure 5b), which means that at pH < 5.86, the surface of UiO-66@Corn⁺ is positively charged. There

is electrostatic attraction between the UiO-66@Corn⁺ and Cr(VI). At pH > 5.86, the surface of UiO-66@Corn⁺ is negatively charged. There is electrostatic repulsion between UiO-66@Corn⁺ and Cr(VI). When the pH of the solution is 5–9, although the equilibrium adsorption capacity of Cr(VI) decreases, it still maintains at a relatively high level, suggesting that in addition to electrostatic attraction, there is also other adsorption force. At pH > 10, the equilibrium adsorption capacity of Cr(VI) dropped sharply. This is because the increased OH⁻ concentration in the solution competes with Cr(VI) for adsorption sites while the electrostatic repulsion between UiO-66@Corn⁺ and Cr(VI) increases. In this study, the optimal pH range for Cr(VI) adsorption by UiO-66@Corn⁺ is 4–6.

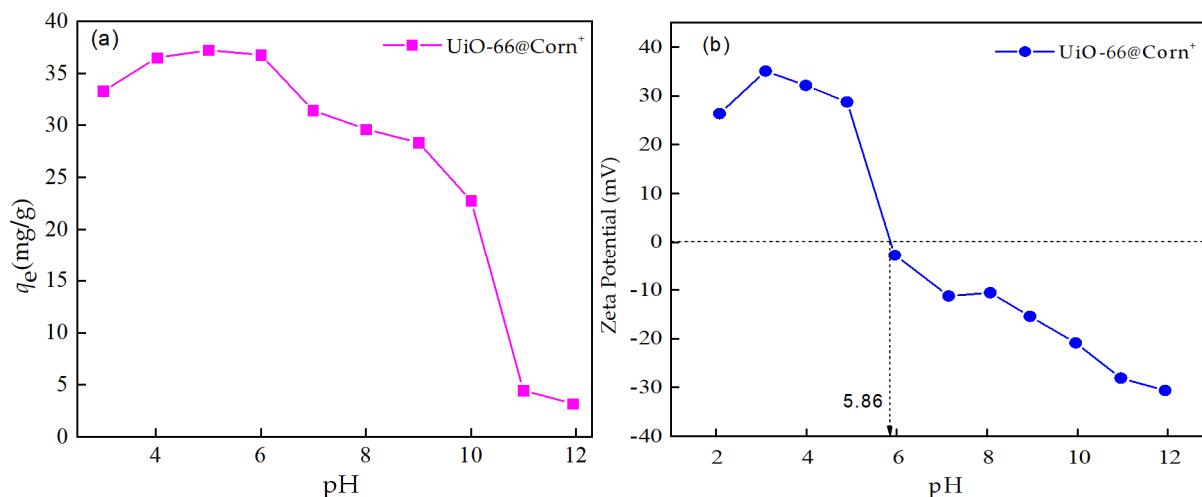


Figure 5. Effects of pH values on the adsorption of Cr(VI) by UiO-66@Corn⁺ (a) and Zeta potentials of UiO-66@Corn⁺ (b).

The effects of ionic strength and coexisting anions such as NO₃⁻, CO₃²⁻, SO₄²⁻ and PO₄³⁻ on the adsorption of Cr(VI) by UiO-66@Corn⁺ were studied. As the ionic strength of the solution increased, the equilibrium adsorption capacity of Cr(VI) first decreased to 0.1 mol/L and then increased (Figure 6a) with the minimal and maximum being 21.60 mg/g and 26.01 mg/g, respectively. Among the coexisting anions, except for Cl⁻ and NO₃⁻, the other three common anions significantly reduce the equilibrium adsorption capacity of Cr(VI). The influence of CO₃²⁻, SO₄²⁻ and PO₄³⁻ on the equilibrium adsorption capacity of Cr(VI) is mainly due to competition for surface adsorption sites. However, the influence of CO₃²⁻ on Cr(VI) adsorption exceeds SO₄²⁻ and PO₄³⁻ (Figure 6b). This phenomenon may be the result of the released OH⁻ from the hydrolysis of CO₃²⁻ ions that causes the solution pH to increase and decreases Cr(VI) equilibrium adsorption capacity. In addition, Zr has a greater affinity for OH⁻, so CO₃²⁻ and OH⁻ can compete with Cr(VI) for adsorption sites [44]. CO₃²⁻, SO₄²⁻ and PO₄³⁻ in the water body can significantly reduce the equilibrium adsorption capacity of Cr(VI). Further research on the selective adsorption of Cr(VI) in complex water environments is needed.

3.5. Regeneration Studies

Reusability is an important factor for evaluating the performance of adsorbents. In this work, the desorption of Cr(VI) for Corn⁺ and UiO-66@Corn⁺ was evaluated with 0.01, 0.1 and 0.5 mol/L NaOH solutions. The adsorption capacity of Cr(VI) on Corn⁺ and UiO-66@Corn⁺ both decreased with NaOH concentration and increased from 0.01 mol/L to 0.5 mol/L (Figure 7a). Thus, the 0.01 mol/L NaOH solution was chosen as the eluant. The adsorption performance of Corn⁺ for Cr(VI) clearly decreased with an increase of adsorption cycles. After five cycles, Corn⁺ only retained 35.58% of its initial Cr(VI) adsorption capacity. The UiO-66@Corn⁺ could be utilized for up to five cycles without any loss of their Cr(VI) adsorption capacity (Figure 7b). These results revealed that the UiO-66@Corn⁺ had excellent regeneration and recycling efficiencies.

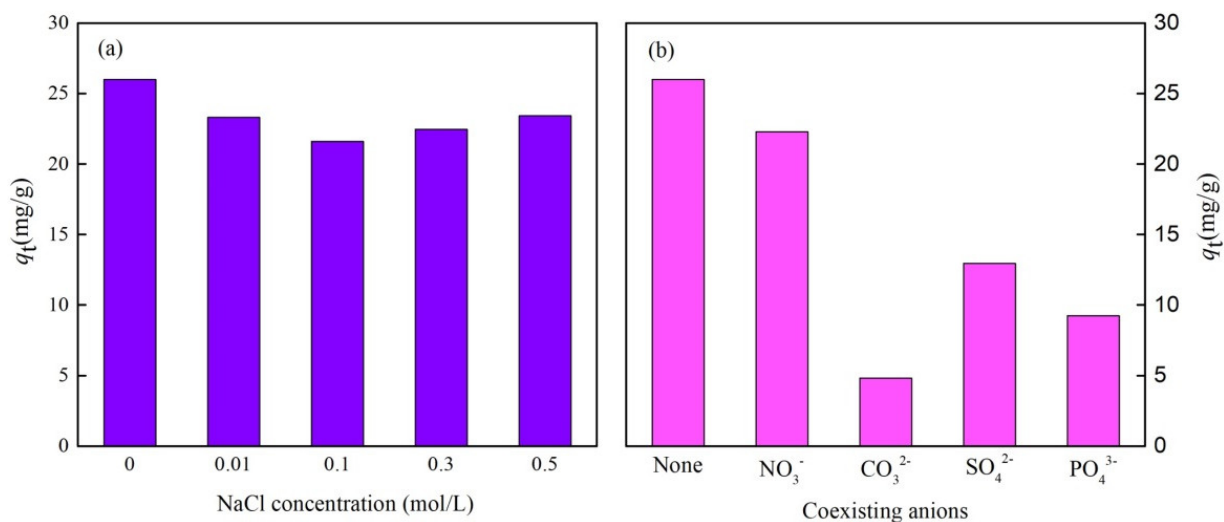


Figure 6. Effects of the ionic strength (a) and the co-existing anions (b) on the adsorption of Cr(VI) by UiO-66@Corn⁺.

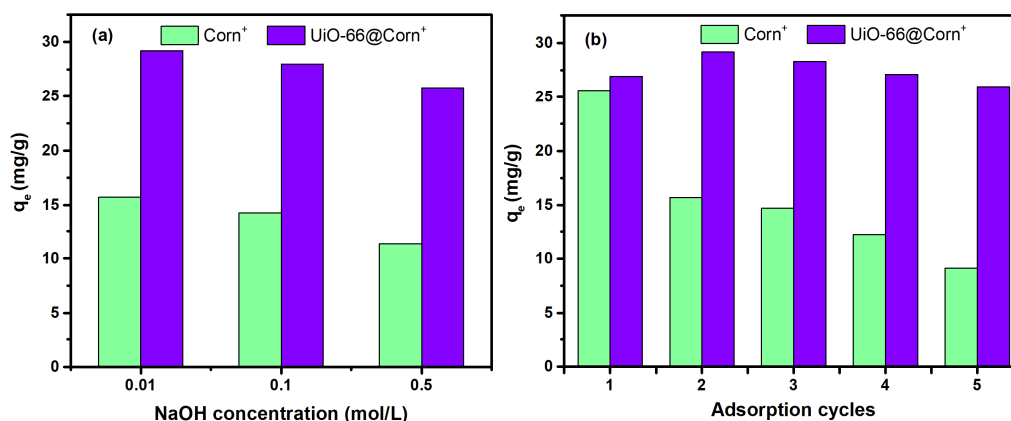


Figure 7. Regeneration studies of Corn⁺ and UiO-66@Corn⁺. (a) The influence of NaOH concentration on adsorbents regeneration; (b) Adsorption-desorption experiment of Cr(VI) on corn⁺ and UiO-66@Corn⁺.

3.6. Adsorption Mechanism of Cr(VI)

As shown in Figure 5b, the point of zero charge (pH_{zpc}) of UiO-66@Corn⁺ was 5.86. The adsorption capacity of UiO-66@Corn⁺ changes with the pH value of the solution and the zeta potential distribution of UiO-66@Corn⁺ changes with pH are highly consistent. As the surface electronegativity of UiO-66@Corn⁺ increases, the adsorption capacity of chromium on UiO-66@Corn⁺ decreases. The significantly decreasing adsorption capacity of Cr(VI) on UiO-66@Corn⁺ with the solution's increasing pH indicated that electrostatic attraction played a leading role in the adsorption process of Cr(VI) and the surface charge of the adsorbent was critical to the adsorption capacity. It is speculated that electrostatic attraction plays an essential role for Cr(VI) adsorption on UiO-66@Corn⁺, which is consistent with the conclusions of previous studies [34,45].

The adsorption mechanism was further evaluated by FTIR analysis (Figure 8). The broad peak that appeared at 3340–3349 cm^{-1} was attributed to stretching vibrations of O-H. The band at 1650 cm^{-1} was assigned to stretching vibrations of C=O. The bands at 1050 cm^{-1} , 1380 cm^{-1} and 1260 cm^{-1} were attributed to stretching vibration of C-O-C, bending vibration of O-H and stretching vibration of C-NH₂, respectively. Both bands at 747 cm^{-1} and 664 cm^{-1} corresponded to the stretching vibration of Zr-O. Above analysis shows there are abundant hydroxyl, amino and other oxygen-containing functional groups on the surface of the UiO-66 modified corncob. Compared to UiO-66@Corn⁺ and UiO-66@Corn⁻, the band at 1380 cm^{-1} of used UiO-66@Corn⁺ and used UiO-66@Corn⁻

became stronger, which was not found on Corn^+ . This might be caused by the abundant unsaturated coordination sites of Zr, which make the $\text{Zr}_6\text{O}_4(\text{OH})_4$ node protonated to $[\text{Zr}_6(\text{OH})_8]^{4+}$ in an acidic environment and offers more $-\text{OH}$ adsorption sites for Cr(VI) adsorption [46]. The band at 1260 cm^{-1} was weakened after adsorption, indicating that $\text{C}-\text{NH}_2$ was consumed in the adsorption process. The fresh peak on used UiO-66@Corn^+ and used Corn^+ appearing at 803 cm^{-1} was the characteristics of Cr(III)-OH [47], which indicates that Cr(VI) was reduced to Cr(III) and the Cr(III) was adsorbed by the $-\text{OH}$ on UiO-66@Corn^+ . It can be speculated from FTIR that the Cr(VI) was adsorbed on the surface of adsorbents through electrostatic attraction and then was reduced to Cr(III) by the electron donor on the surface of adsorbent [30]. The FTIR results indicated that the hydroxyl groups and amino on the surface of adsorbents played an important role during Cr(VI) adsorption. It was speculated that Cr(VI) was reduced by the electron donor on the surface of adsorbent such as the lone pair electrons on hydroxyl and amino on Corn^+ .

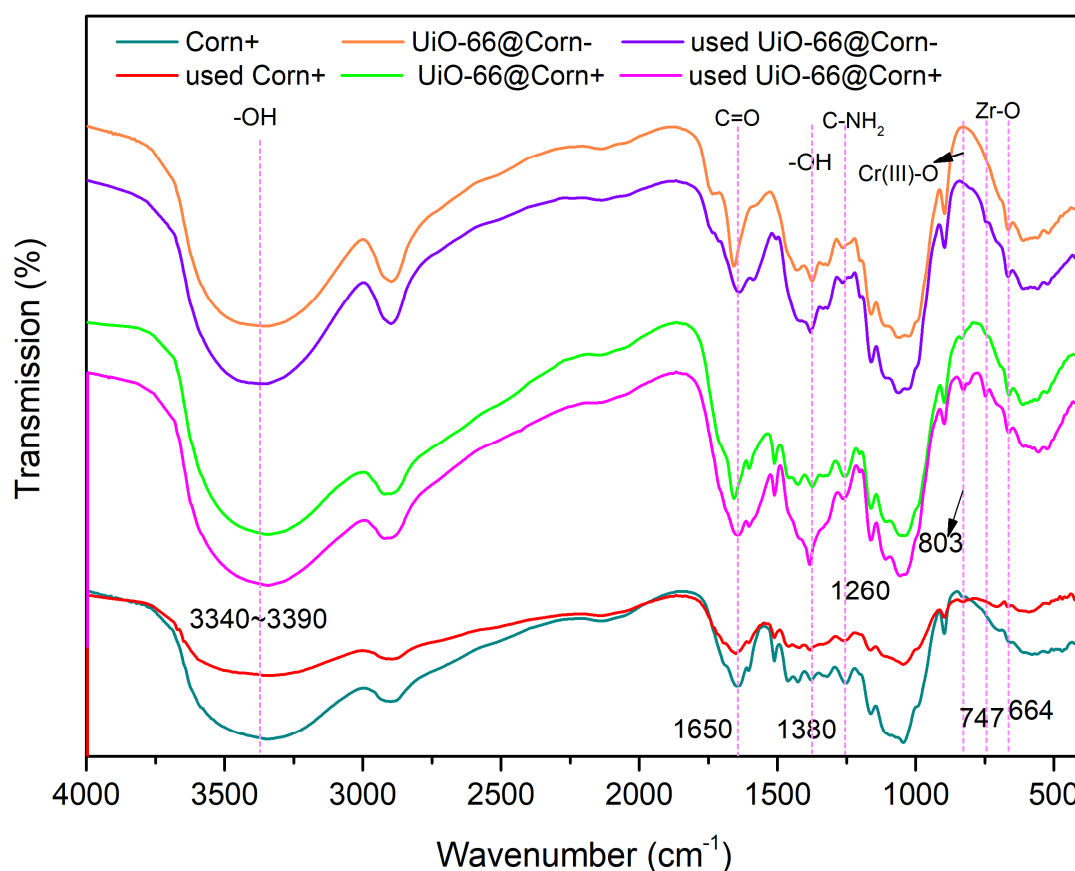


Figure 8. FTIR patterns of the adsorbents before and after Cr(VI) adsorption.

The XPS full spectrum analysis (Figure 9a) showed that UiO-66 modified corncob only had four elements: Zr, O, N and C before adsorption. After adsorption, a new peak at 575 eV appeared as Cr2p, confirming that Cr was successfully adsorbed on the UiO-66 modified corncob. The narrow scan of O showed that the content of $-\text{OH}$ increased after Cr(VI) adsorption (Figure 9b), which was consistent with the FTIR result. This could be due to the $\text{Zr}_6\text{O}_4(\text{OH})_4$ node being protonated to $[\text{Zr}_6(\text{OH})_8]^{4+}$ in the acidic environment [46]. The $-\text{OH}$ could be protonated $-\text{OH}_2^+$ in the acidic solution, which could increase the electrostatic attraction and promote Cr(VI) adsorption [47]. During Cr(VI) adsorption, Zr content on corncob remained unchanged (Figure 9c), indicating that the UiO-66 was very stable and there was no exchange of Zr with Cr during adsorption. According to the XPS peak splitting spectrum (Figure 9d–f), the Cr2p spectrum was further decomposed into Cr(VI) (579.6 eV, 588.9 eV) and Cr(III) (577.5 eV, 586.6 eV) [45]. The Cr(VI) and

Cr(III) accounted for 38.4% and 61.6% on used UiO-66@Corn⁺, respectively. This shows that the adsorption of Cr(VI) on UiO-66@Corn⁺ existed in both physical adsorption and chemisorption. Additionally, it was also confirmed Cr(VI) is reduced to Cr(III) by the electron donor on the surface of UiO-66@Corn⁺ during the adsorption process [48]. Only Cr(III) existed on used UiO-66@Corn⁻ (Figure 9e) and used Corn⁺ (Figure 9f), indicating that the adsorption of Cr(VI) by UiO-66@Corn⁻ and used Corn⁺ was mainly chemisorption. The intensity of the Cr(VI) and Cr(III) peaks on used UiO-66@Corn⁻ was much less than on used UiO-66@Corn⁺, indicating that the loading content of Cr by UiO-66@Corn⁺ was much greater than UiO-66@Corn⁻.

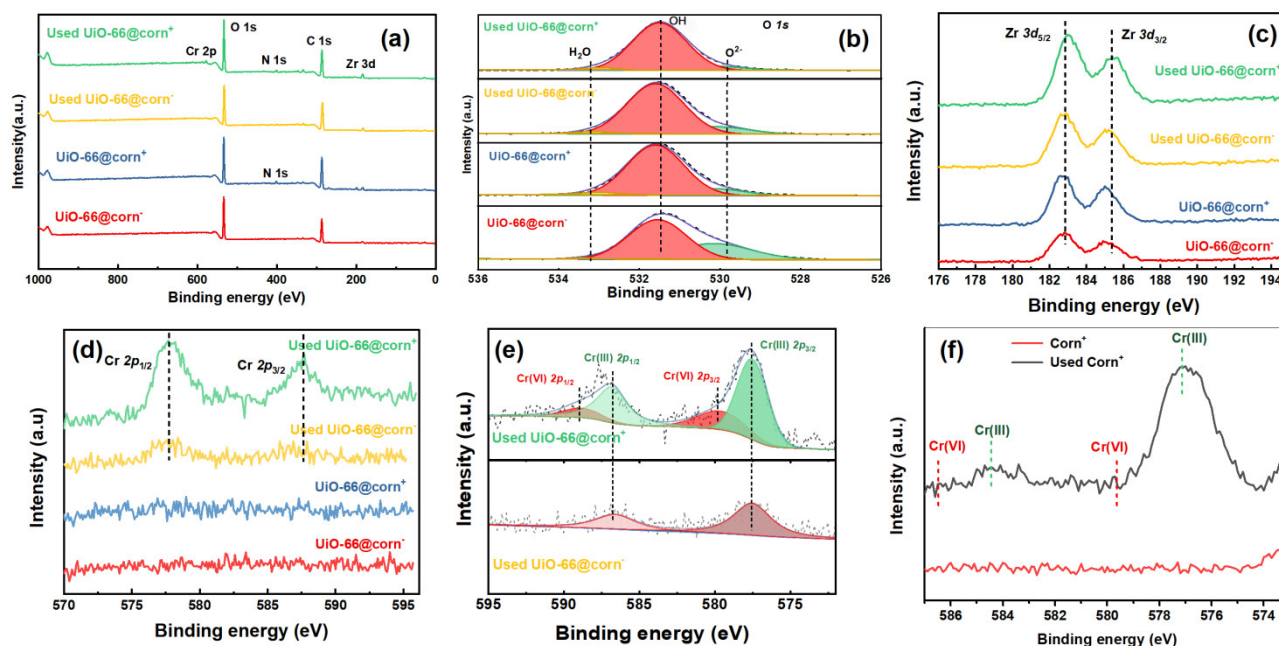


Figure 9. XPS scan spectra of UiO-66 modified corncob before and after Cr(VI) adsorption: (a) full range, (b) O1s, (c) Zr3d, (d–f) Cr2p.

4. Conclusions

In this study, two kinds of UiO-66 modified granular corncob composite adsorbents were prepared by a hydrothermal method, and their removal process of Cr(VI) in water was studied. Compared with UiO-66@Corn⁻, UiO-66@Corn⁺ was more porous and loaded by more UiO-66 particles. The adsorption isotherm experiment data fit well with the Langmuir isotherm model. The maximum adsorption capacities of Cr(VI) on UiO-66, Corn⁺, UiO-66@Corn⁺ and UiO-66@Corn⁻ were 109.88 mg/g, 60.232 mg/g, 90.038 mg/g and 22.383 mg/g, respectively. UiO-66 loading can significantly increase the adsorption capacity of Cr(VI) by Corn⁺. The adsorption kinetics of Cr(VI) followed the pseudo-second-order kinetic model, proposing that the adsorption process tended to be chemical adsorption and the equilibrium time was 180 min. The optimal pH range for UiO-66@Corn⁺ to adsorb Cr(VI) was 4–6. Bivalent and trivalent anions that coexisted in the solution can significantly reduce the equilibrium adsorption capacity of Cr(VI). Electrostatic attraction was the main force for Cr(VI) adsorption, and most of Cr(VI) was reduced to Cr(III) during the adsorption process, which could reduce the toxicity of chromium. Further research on the selective adsorption of Cr(VI) in complex water environments is needed. The hydroxyl groups and amino on the surface of adsorbents played an important role during Cr(VI) adsorption. UiO-66 modified corncob exhibited enhanced adsorption capacity, Cr(VI) specific adsorption and reusability, compared to virgin corncob and Corn⁺. These results additionally provided new insight into resource utilization of agricultural waste as well as adsorption by MOFs.

Supplementary Materials: The following are available online at <https://www.mdpi.com/article/10.3390/su132312962/s1>, Table S1: Percentage of elements from EDS in the samples.

Author Contributions: Conceptualization, resources and writing—review and editing, Q.Z.; writing—original draft preparation, H.X. and Y.W.; data curation, H.C.; supervision, L.W. and Q.X.; visualization, X.L.; formal analysis, G.X.; investigation, Q.Z., H.X., Y.W. and H.C. All authors have read and agreed to the published version of the manuscript.

Funding: This work was financially supported by the Key Research and Development Program of Hubei Province (2020BCA073), Technology Demonstration Program of Water Resources (SF-202009), Independent Innovation Research Program of Changjiang Survey, Planning, Design and Research Co., Ltd. (CX2020Z23) and China Postdoctoral Science Foundation (2021M692753).

Institutional Review Board Statement: Not applicable.

Informed Consent Statement: Not applicable.

Data Availability Statement: Data is contained within this article.

Conflicts of Interest: The authors declare no conflict of interest.

References

1. Ihsanullah; Abbas, A.; Al-Amer, A.M.; Laoui, T.; Al-Marri, M.J.; Nasser, M.S.; Khraisheh, M.; Atieh, M. Heavy metal removal from aqueous solution by advanced carbon nanotubes: Critical review of adsorption applications. *Sep. Purif. Technol.* **2016**, *157*, 141–161. [[CrossRef](#)]
2. Rego, R.M.; Sriram, G.; Ajeya, K.V.; Jung, H.-Y.; Kurkuri, M.D.; Kigga, M. Cerium based UiO-66 MOF as a multipollutant adsorbent for universal water purification. *J. Hazard. Mater.* **2021**, *416*, 125941. [[CrossRef](#)] [[PubMed](#)]
3. Chen, Q.; Feng, Y.; Tian, R.; Chen, J.; Wang, A.; Yao, J. Defect Rich UiO-66 with Enhanced Adsorption and Photosensitized Reduction of Cr(VI) under Visible Light. *Ind. Eng. Chem. Res.* **2019**, *58*, 21562–21568. [[CrossRef](#)]
4. Thach, U.D.; Prelot, B.; Pellet-Rostaing, S.; Zajac, J.; Hesemann, P. Surface Properties and Chemical Constitution as Crucial Parameters for the Sorption Properties of Ionosilicas: The Case of Chromate Adsorption. *ACS Appl. Nano Mater.* **2018**, *1*, 2076–2087. [[CrossRef](#)]
5. Burakov, A.; Galunin, E.V.; Burakova, I.V.; Kucherova, A.; Agarwal, S.; Tkachev, A.G.; Gupta, V.K. Adsorption of heavy metals on conventional and nanostructured materials for wastewater treatment purposes: A review. *Ecotoxicol. Environ. Saf.* **2018**, *148*, 702–712. [[CrossRef](#)] [[PubMed](#)]
6. Wang, P.; Du, M.; Zhu, H.; Bao, S.; Yang, T.; Zou, M. Structure regulation of silica nanotubes and their adsorption behaviors for heavy metal ions: pH effect, kinetics, isotherms and mechanism. *J. Hazard. Mater.* **2015**, *286*, 533–544. [[CrossRef](#)]
7. Fiyadh, S.S.; AlSaadi, M.A.; Jaafar, W.Z.; AlOmar, M.; Fayaed, S.S.; Mohd, N.S.; Hin, L.S.; El-Shafie, A. Review on heavy metal adsorption processes by carbon nanotubes. *J. Clean. Prod.* **2019**, *230*, 783–793. [[CrossRef](#)]
8. Bhadra, B.N.; Lee, J.K.; Cho, C.-W.; Jhung, S.H. Remarkably efficient adsorbent for the removal of bisphenol A from water: Bio-MOF-1-derived porous carbon. *Chem. Eng. J.* **2018**, *343*, 225–234. [[CrossRef](#)]
9. Xu, G.-R.; An, Z.-H.; Xu, K.; Liu, Q.; Das, R.; Zhao, H.-L. Metal organic framework (MOF)-based micro/nanoscaled materials for heavy metal ions removal: The cutting-edge study on designs, synthesis, and applications. *Coord. Chem. Rev.* **2020**, *427*, 213554. [[CrossRef](#)]
10. Wang, C.; Luan, J.; Wu, C. Metal-organic frameworks for aquatic arsenic removal. *Water Res.* **2019**, *158*, 370–382. [[CrossRef](#)]
11. Li, Y.; Fang, Y.; Cao, Z.; Li, N.; Chen, D.; Xu, Q.; Lu, J. Construction of g-C₃N₄/PDI@MOF heterojunctions for the highly efficient visible light-driven degradation of pharmaceutical and phenolic micropollutants. *Appl. Catal. B Environ.* **2019**, *250*, 150–162. [[CrossRef](#)]
12. Zhang, J.; Xu, X.; Chen, L. An ultrasensitive electrochemical bisphenol A sensor based on hierarchical Ce-metal-organic framework modified with cetyltrimethylammonium bromide. *Sens. Actuators B Chem.* **2018**, *261*, 425–433. [[CrossRef](#)]
13. Ahmad, K.; Shah, H.-U.-R.; Ashfaq, M.; Nawaz, H. Removal of decidedly lethal metal arsenic from water using metal organic frameworks: A critical review. *Rev. Inorg. Chem.* **2021**. accepted. [[CrossRef](#)]
14. Dhakshinamoorthy, A.; Santiago-Portillo, A.; Asiri, A.M.; Garcia, H. Engineering UiO-66 Metal Organic Framework for Heterogeneous Catalysis. *ChemCatChem* **2019**, *11*, 899–923. [[CrossRef](#)]
15. Audu, C.O.; Nguyen, H.G.T.; Chang, C.-Y.; Katz, M.J.; Mao, L.; Farha, O.K.; Hupp, J.T.; Nguyen, S.T. The dual capture of AsV and AsIII by UiO-66 and analogues. *Chem. Sci.* **2016**, *7*, 6492–6498. [[CrossRef](#)] [[PubMed](#)]
16. Li, L.-L.; Feng, X.-Q.; Han, R.-P.; Zang, S.-Q.; Yang, G. Cr(VI) removal via anion exchange on a silver-triazolate MOF. *J. Hazard. Mater.* **2017**, *321*, 622–628. [[CrossRef](#)]
17. Sun, X.; Yao, S.; Yu, C.; Li, G.; Liu, C.; Huo, Q.; Liu, Y. An ultrastable Zr-MOF for fast capture and highly luminescence detection of Cr₂O₇²⁻—simultaneously in an aqueous phase. *J. Mater. Chem. A* **2018**, *6*, 6363–6369. [[CrossRef](#)]

18. Duan, C.; Meng, X.; Liu, C.; Lu, W.; Liu, J.; Dai, L.; Wang, W.; Zhao, W.; Xiong, C.; Ni, Y. Carbohydrates-rich corncoobs supported metal-organic frameworks as versatile biosorbents for dye removal and microbial inactivation. *Carbohydr. Polym.* **2019**, *222*, 115042. [[CrossRef](#)]
19. Yan, B.; Yan, J.; Li, Y.; Qin, Y.; Yang, L. Spatial distribution of biogas potential, utilization ratio and development potential of biogas from agricultural waste in China. *J. Clean. Prod.* **2021**, *292*, 126077. [[CrossRef](#)]
20. Qiu, H.; Ye, M.; Zeng, Q.; Li, W.; Fortner, J.; Liu, L.; Yang, L. Fabrication of agricultural waste supported UiO-66 nanoparticles with high utilization in phosphate removal from water. *Chem. Eng. J.* **2019**, *360*, 621–630. [[CrossRef](#)]
21. Ahmad, K.; Shah, H.-U.-R.; Nasim, H.A.; Ayub, A.; Ashfaq, M.; Rauf, A.; Shah, S.S.A.; Ahmad, M.M.; Nawaz, H.; Hussain, E. Synthesis and characterization of water stable polymeric metallo organic composite (PMOC) for the removal of arsenic and lead from brackish water. *Toxin Rev.* **2021**, *40*. [[CrossRef](#)]
22. Ahmad, K.; Nazir, M.A.; Qureshi, A.K.; Hussain, E.; Najam, T.; Javed, M.S.; Shah, S.S.A.; Tufail, M.K.; Hussain, S.; Khan, N.A.; et al. Engineering of Zirconium based metal-organic frameworks (Zr-MOFs) as efficient adsorbents. *Mater. Sci. Eng. B* **2020**, *262*, 114766. [[CrossRef](#)]
23. Ahmad, K.; Shah, H.-U.-R.; Ashfaq, M.; Shah, S.S.A.; Hussain, E.; Naseem, H.A.; Parveen, S.; Ayub, A. Effect of metal atom in zeolitic imidazolate frameworks (ZIF-8 & 67) for removal of Pb²⁺ & Hg²⁺ from water. *Food Chem. Toxicol.* **2021**, *149*, 112008. [[CrossRef](#)]
24. Shah, H.U.R.; Ahmad, K.; Naseem, H.A.; Parveen, S.; Ashfaq, M.; Rauf, A.; Aziz, T. Water stable graphene oxide metal-organic frameworks composite (ZIF-67@GO) for efficient removal of malachite green from water. *Food Chem. Toxicol.* **2021**, *154*, 112312. [[CrossRef](#)] [[PubMed](#)]
25. Ahmad, K.; Shah, H.-U.-R.; Parveen, S.; Aziz, T.; Naseem, H.A.; Ashfaq, M.; Rauf, A. Metal Organic Framework (KIUB-MOF-1) as Efficient Adsorbent for Cationic and Anionic Dyes from Brackish Water. *J. Mol. Struct.* **2021**, *1242*, 130898. [[CrossRef](#)]
26. Ayub, A.; Irfan, A.; Raza, Z.A.; Abbas, M.; Muhammad, A.; Ahmad, K.; Munwar, A. Development of poly(1-vinylimidazole)-chitosan composite sorbent under microwave irradiation for enhanced uptake of Cd(II) ions from aqueous media. *Polym. Bull.* **2021**. [[CrossRef](#)]
27. Katz, M.J.; Brown, Z.J.; Colón, Y.J.; Siu, P.W.; Scheidt, K.A.; Snurr, R.Q.; Hupp, J.T.; Farha, O.K. A facile synthesis of UiO-66, UiO-67 and their derivatives. *Chem. Commun.* **2013**, *49*, 9449–9451. [[CrossRef](#)] [[PubMed](#)]
28. Tan, K.; Hameed, B. Insight into the adsorption kinetics models for the removal of contaminants from aqueous solutions. *J. Taiwan Inst. Chem. Eng.* **2017**, *74*, 25–48. [[CrossRef](#)]
29. Wu, F.-C.; Tseng, R.-L.; Juang, R.-S. Initial behavior of intraparticle diffusion model used in the description of adsorption kinetics. *Chem. Eng. J.* **2009**, *153*, 1–8. [[CrossRef](#)]
30. Guo, X.; Liu, A.; Lu, J.; Niu, X.; Jiang, M.; Ma, Y.; Liu, X.; Li, M. Adsorption Mechanism of Hexavalent Chromium on Biochar: Kinetic, Thermodynamic, and Characterization Studies. *ACS Omega* **2020**, *5*, 27323–27331. [[CrossRef](#)]
31. Liu, S.S.; Chen, Y.Z.; De Zhang, L.; Hua, G.M.; Xu, W.; Li, N.; Zhang, Y. Enhanced removal of trace Cr(VI) ions from aqueous solution by titanium oxide–Ag composite adsorbents. *J. Hazard. Mater.* **2011**, *190*, 723–728. [[CrossRef](#)]
32. Deng, Y.-Y.; Xiao, X.-F.; Wang, D.; Han, B.; Gao, Y.; Xue, J.-L. Adsorption of Cr(VI) from Aqueous Solution by Ethylenediaminetetraacetic Acid–Chitosan-Modified Metal-Organic Framework. *J. Nanosci. Nanotechnol.* **2020**, *20*, 1660–1669. [[CrossRef](#)]
33. Periyasamy, S.; Viswanathan, N. Hydrothermal synthesis of hydrocalumite assisted biopolymeric hybrid composites for efficient Cr(vi) removal from water. *New J. Chem.* **2018**, *42*, 3371–3382. [[CrossRef](#)]
34. Wang, Z.; Yang, J.; Li, Y.; Zhuang, Q.; Gu, J. Simultaneous Degradation and Removal of CrVI from Aqueous Solution with Zr-Based Metal-Organic Frameworks Bearing Inherent Reductive Sites. *Chem. Eur. J.* **2017**, *23*, 15415–15423. [[CrossRef](#)]
35. Mukri, B.; Krushnamurthy, K.; Chowdhury, A.; Suryakala, D.; Subrahmanyam, C. Alkali-treated Carbonized Rice Husk for the Removal of Aqueous Cr(VI). *BioResources* **2016**, *11*, 9175–9189. [[CrossRef](#)]
36. Zheng, Y.Q.; Cheng, B.; You, W.; Yu, J.G.; Ho, W.K. 3D hierarchical graphene oxide-NiFe LDH composite with enhanced adsorption affinity to Congo red, methyl orange and Cr(VI) ions. *J. Hazard. Mater.* **2019**, *369*, 214–225. [[CrossRef](#)] [[PubMed](#)]
37. Bao, D.; Wang, H.; Liao, W.; Li, H.-Q. Multi-Metal Modified Layered Double Hydroxides for Cr(VI) and Fluoride Ion Adsorption in Single and Competitive Systems: Experimental and Mechanism Studies. *Environ. Eng. Sci.* **2020**, *37*, 623–636. [[CrossRef](#)]
38. Jin, X.; Wang, H.J.; Jin, X.; Wang, H.; Chen, L.N.; Wang, W.Y.; Lin, T.; Zhu, Z.T. Preparation of keratin/PET nanofiber membrane and its high adsorption performance of Cr(VI). *Sci. Total Environ.* **2020**, *710*, 135546. [[CrossRef](#)]
39. Hoang, L.P.; Nguyen, T.M.P.; Van, H.T.; Hoang, T.K.D.; Vu, X.H.; Nguyen, T.V.; Ca, N.X. Cr(VI) Removal from Aqueous Solution Using a Magnetite Snail Shell. *Water Air Soil Pollut.* **2020**, *231*, 28. [[CrossRef](#)]
40. Zhang, Q.; Yu, J.; Cai, J.; Zhang, L.; Cui, Y.; Yang, Y.; Chen, B.; Qian, G. A porous Zr-cluster-based cationic metal-organic framework for highly efficient Cr₂O₇²⁻ removal from water. *Chem. Commun.* **2015**, *51*, 14732–14734. [[CrossRef](#)]
41. Du, Y.; Wang, L.; Wang, J.; Zheng, G.; Wu, J.; Dai, H. Flower-, wire-, and sheet-like MnO₂-deposited diatomites: Highly efficient adsorbents for the removal of Cr(VI). *J. Environ. Sci.* **2015**, *29*, 71–81. [[CrossRef](#)]
42. Liu, S.; Chen, M.; Cao, X.; Li, G.; Zhang, D.; Li, M.; Meng, N.; Yin, J.; Yan, B. Chromium (VI) removal from water using cetylpyridinium chloride (CPC)-modified montmorillonite. *Sep. Purif. Technol.* **2020**, *241*, 116732. [[CrossRef](#)]
43. Yang, J.; Huang, B.; Lin, M. Adsorption of Hexavalent Chromium from Aqueous Solution by a Chitosan/Bentonite Composite: Isotherm, Kinetics, and Thermodynamics Studies. *J. Chem. Eng. Data* **2020**, *65*, 2751–2763. [[CrossRef](#)]

44. Wang, L.; Xie, Y.; Yang, J.; Zhu, X.; Hu, Q.; Li, X.; Liu, Z. Insight into mechanisms of fluoride removal from contaminated groundwater using lanthanum-modified bone waste. *RSC Adv.* **2017**, *7*, 54291–54305. [[CrossRef](#)]
45. Wang, Y.; Zhang, N.; Chen, D.; Ma, D.; Liu, G.; Zou, X.; Chen, Y.; Shu, R.; Song, Q.; Lv, W. Facile synthesis of acid-modified UiO-66 to enhance the removal of Cr(VI) from aqueous solutions. *Sci. Total Environ.* **2019**, *682*, 118–127. [[CrossRef](#)] [[PubMed](#)]
46. Embaby, M.S.; Elwany, S.D.; Setyaningsih, W.; Saber, M.R. The adsorptive properties of UiO-66 towards organic dyes: A record adsorption capacity for the anionic dye Alizarin Red S. *Chin. J. Chem. Eng.* **2018**, *26*, 731–739. [[CrossRef](#)]
47. Jiang, Y.; Cai, W.; Tu, W.; Zhu, M. Facile Cross-Link Method To Synthesize Magnetic Fe₃O₄@SiO₂-Chitosan with High Adsorption Capacity toward Hexavalent Chromium. *J. Chem. Eng. Data* **2018**, *64*, 226–233. [[CrossRef](#)]
48. Wang, C.; Xiong, C.; He, Y.; Yang, C.; Li, X.; Zheng, J.; Wang, S. Facile preparation of magnetic Zr-MOF for adsorption of Pb(II) and Cr(VI) from water: Adsorption characteristics and mechanisms. *Chem. Eng. J.* **2021**, *415*, 128923. [[CrossRef](#)]